

Anisotropic diffusion of radiation-induced self-interstitial clusters in HCP zirconium: a molecular dynamics and rate-theory assessment

Amir Ghorbani^a, Yu Luo^a, Peyman Saidi^{a,b}, Laurent Karim Béland^{a,*}

^aDepartment of Mechanical and Materials Engineering, Queen's University, Kingston, ON K7L3N6, Canada

^bCanadian Nuclear Laboratories, Chalk River, ON K0J 1J0, Canada

Abstract

Under irradiation, Zr and Zr alloys undergo growth in the absence of applied stress. This phenomenon is thought to be associated with the anisotropy of diffusion of either or both radiation-induced point defects and defect clusters. In this work, molecular dynamic simulations are used to study the anisotropy of diffusion of self-interstitial atom clusters. Both near-equilibrium clusters generated by aggregation of self-interstitial atoms and cascade-induced clusters were considered. The cascade-induced clusters display more anisotropy than their counterparts produced by aggregation. In addition to 1-dimensional diffusing clusters, 2-dimensional diffusing clusters were observed. Using our molecular dynamic simulations, the input parameters for the "self-interstitial atom cluster bias" rate-theory model were estimated. The radiation-induced growth strains predicted using this model are largely consistent with experiments, but are highly sensitive to the choice of interatomic interaction potential.

Keywords: Irradiation, Radiation Induced Growth, Cluster, Zirconium, Molecular Dynamics

HCP metals such as Mg, Ti and Zr – and their alloys – grow when exposed to high-energy particle irradiation. Radiation-induced growth (RIG) is volume conservative; it develops in the absence of applied stress and involves expansion in the prismatic (a) directions and contraction in the basal (c) axis. This transformation, unique to HCP materials, can be problematic in the context of nuclear power applications, since Zr alloys are widely used as fuel cladding materials in most commercial reactors and also as structural materials in CANDU (CANadian Deuterium Uranium) reactors due to their low neutron absorption cross-section [1, 2, 3, 4, 5, 6, 7]. Despite decades of research, the physical nature of the micro-mechanisms explaining RIG remains unclear.

Linking macroscopic RIG and microscopic defect evolution has been the topic of multiple theoretical efforts in the past 60 years [8, 9, 10, 11, 12, 13]. Two leading theories, the Difference in Anisotropy of Diffusion (DAD) [9] model and the self-interstitial

atom cluster bias (SIACB) [13] model are based on the assumption of anisotropic mass transport. Specifically, they both require that interstitial-type defects diffuse primarily along prismatic directions. This anisotropy in turn influences defect-defect and defect-sink interactions. Namely, it suppresses the growth of vacancy-type prismatic dislocation loops (a-loops) and interstitial-type c-loops and promotes the growth of interstitial-type a-loops and vacancy-type c-loops. The main difference between these models is that self-interstitial atoms (SIAs) are the agent of anisotropy in DAD while one-dimensional (1-D) gliding SIA clusters also play a major role in SIACB. Note that both models assume that c-loops appear once a certain radiation dose is reached, without providing micro-mechanistic explanations for this behaviour. The origin of vacancy c-loops formation has been the topic of numerous experimental and theoretical scientific studies [7, 14, 15, 16, 17]. Plausible explanations include the growth of small planar basal vacancy platelets into c-loops and cascade-induced collapse of multiple a-loops lying on the same basal plane into a c-loop [18].

Within the DAD framework, the SIA's diffusional

*Corresponding author

Email address: laurent.beland@queensu.ca (Laurent Karim Béland)

anisotropy D_a/D_c is assumed to be more than a hundred times larger than the vacancy's. However, *ab initio* calculations by Samolyuk *et al.* suggest that the difference in diffusional anisotropy between SIAs and vacancies in Zr is not as large as that required by this model; in fact, the calculations suggest it may have the wrong sign [11]. In SIACB, large D_a/D_c of self-interstitial defects is explained not by the anisotropy of diffusion of point defects, but rather by the anisotropy of diffusion of 1D gliding clusters. In this model, the growth rate is controlled by ε_i^g , the ratio of 1-D gliding SIA clusters to total SIAs, and n_i^g , the mean number of SIAs in these clusters. Previous molecular modelling—using older force-fields—indicates that glissile SIA clusters can be produced by collision cascades in Zr [19, 20, 21]. Other modelling studies focused on the diffusion behaviour of individual sessile and glissile SIA clusters [22, 23, 24, 25] and of clusters emerging from the aggregation of a large number of point defects [26]. Questions remain as to whether SIA clusters directly generated by collision cascades and aggregation of point defects present the same degree of diffusional anisotropy. Furthermore, the propensity for 1D gliding clusters generation by cascades has not been revisited using more recent force-fields.

In this article, we model and compare the diffusional anisotropy of SIA clusters produced by aggregation with those produced directly by collision cascades (see supplementary material (SM) - sections 3 & 4). First, we re-parametrized two widely used zirconium force-fields at short interatomic distances based on density functional theory (DFT) calculations. Second, the diffusion behaviour of SIA clusters produced by the aggregation of SIAs is presented. Third, the diffusion behaviour of SIA clusters produced in cascades is described. Finally, estimates of ε^g and n^g are reported, and predictions pertaining to growth behaviour using a rate-theory model (i.e. a sensitivity analysis) are provided.

The choice of force-field plays a crucial role in determining the mobility of SIA clusters [25, 24]. Furthermore, primary damage production is highly sensitive to the method chosen to model short-to-mid-distance (1 to 2 Å) interatomic interactions [27, 28, 29, 30, 31]. Here, Mendeleev and Ackland's [32] Zr potentials, referred to here as M2 and M3, were chosen and reparameterized at short interatomic distances following the procedure explained in Ref. [27]. We refer to the reparameterized potentials as M2R and M3R (see SM - section 2). Elastic constants and SIA formation energies were not ma-

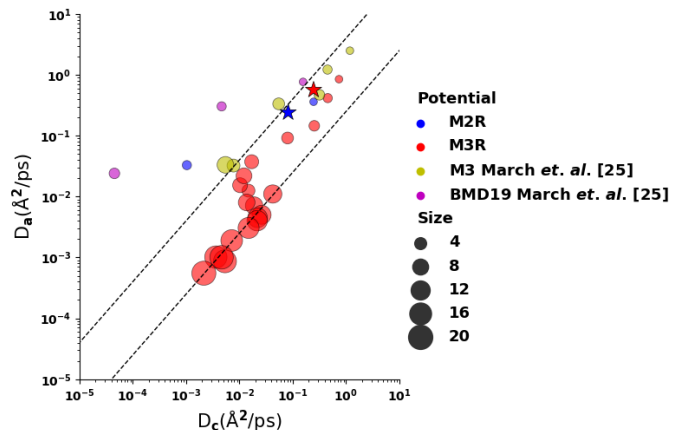


Figure 1: Diffusion coefficients along the basal and prismatic planes of SIA clusters generated by aggregation of SIAs. Here, the circular marker radius is associated with the size of the corresponding SIA cluster, while the stars are single SIAs. Values within the dashed lines exhibit diffusional anisotropy corresponding to a bias factor of less than 25%. We also display simulation results from March *et al.* [25], who employed the M3 and BMD19 potentials.

terially affected by this reparametrization.

Using the reparameterized potentials, we performed molecular dynamic (MD) simulations to study SIA clusters produced by aggregation of individual SIAs, comprised of up to 20 SIAs, to track their mobility. Each cluster was simulated for 100 ns at 573K in a box containing more than 15000 atoms using the Large-scale Atomic/Molecular Massively Parallel Simulator (LAMMPS)[33] with a timestep of 1 fs in the NVT ensemble employing a Nosé-Hoover thermostat. SIAs were added to the simulation cell one at a time, allowing them to form a single cluster before adding another (see SM - section 3 and video 1). While M2R SIA clusters tend to form sessile platelets, M3R clusters tend to form glissile configurations.

Diffusion coefficients of these clusters along basal (D_c) and prismatic (D_a) planes were calculated and reported in Fig. 1 (see SM - section 3.2). To distinguish between isotropic and anisotropic behaviour, we chose a D_a to D_c ratio threshold of four, which corresponds to a bias factor of 25%, following the model proposed in Ref. [34] (see SM - section 5). The dashed lines in Fig. 1 bound the diffusion coefficient in the isotropic regime. Most of the clusters diffuse roughly isotropically. Furthermore, diffusivity diminishes as clusters become larger [26]. Instead of forming clusters by aggregation of SIAs, March *et al.* [25] directly introduced crowdion

SIA clusters in their simulation box, using the M3 and BMD19 potentials. Their results are included in the data presented in Fig. 1.

Irradiation of pure Zr was simulated in LAMMPS assuming primary knock-on atom (PKA) energies of 10, 20, 30 and 40 keV at 573K (see SM - section 4 and video 2). 64 equidistributed initial PKA directions were chosen in one-sixth of a sphere for each potential and PKA energy. The simulation boxes contained more than 2.5 million atoms ($140 \times 80 \times 60$ unit cells) and time integration using a variable step size was performed for a duration of 500 ps. No thermostat was applied except for an exterior layer of 2 unit cells where we applied a Langevin thermostat at 573K.

Wigner-Seitz cell analysis (WS) was performed using OVITO [35] to determine the number of Frenkel pairs (FP) present in the simulation cells (see SM - section 4.2). Fig. 2 (a) shows the averaged remaining FPs at the end of the cascade. For comparison, an estimate of FP production based on the athermal recombination corrected displacement per atom (arc-dpa) model is also provided [36, 37]. Note that this arc-dpa estimate is itself fitted on cascades simulated using the non-reparametrized M2 potential [38, 39, 40]. FP production increases in tandem with energy. Cascades simulated using the M2R potential led to a greater amount of FP produced than those performed using M3R. The arc-dpa estimates fall between these values.

Next, cluster analysis was performed using a cut-off distance of 5.8 Å. The size of the SIA clusters remaining at the end of the cascade was averaged and illustrated in Fig. 2 (b). Greater PKA energy results in a slight increase in cluster size. The average SIA cluster size associated with M3R is double that associated with M2R.

To calculate n_i^g and ε_i^g , we analyzed the behaviour of SIA clusters both visually and algorithmically to distinguish different cluster types. Less than 200 1-D gliders were observed in the 256 M2R cascade simulations; when considering M3R, this number is limited to 70. These 1-D clusters were mostly comprised of 6 to 11 SIAs (see SM - section 4.4.1).

Next, the 1-D clusters were visualized using equivalent sphere analysis (see SM - section 8 and video 3) [41]. The common feature of 1-D gliders is consecutive crowdions stacking along the c-axis and seamless arrangement along the a-axis. As shown in Fig. 3 (a) left, six crowdion SIAs form three pairs in basal planes. These crowdions are shown along the

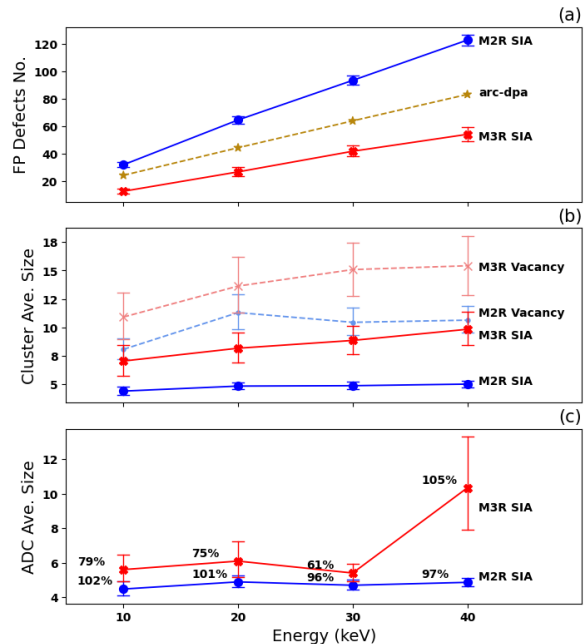


Figure 2: Primary damage production in HCP Zr. In panel (a), we report the total number of displaced atoms as a function of the PKA kinetic energy. 64 MD runs using each force-field were averaged and compared to the predictions of the arc-dpa model. In panel (b), we report the average SIA and vacancy cluster size as a function of the PKA kinetic energy. In panel (c), we report the average size of ADCs (a-biased diffusing clusters) as a function of the PKA kinetic energy in comparison with the average SIA cluster size. Error bars correspond to confidence intervals of 95%.

a-axis in Fig. 3 (a) right. The majority of the clusters show the same symmetric pattern with a different number of crowdions. These clusters move back on forth along $[11\bar{2}0]$ direction, without a change in their nature. Another notable characteristic of the clusters, mainly observed in M3R interatomic potential, was the reconfiguration of crowdions to change the mobility direction from one a-axis to another. This behaviour is illustrated in Fig. 3 (b). These are 2-dimensional (2-D) gliding clusters. Interestingly, such 2D motion of SIA clusters was reported in the past [26, 23], but, to the best of our knowledge, their quantitative impact on RIG has not been assessed. At the moment of transition, crowdions move out of the plane and rearrange to form crowdions in an alternative $\langle 11\bar{2}0 \rangle$ direction. These are a-biased diffusing clusters, which should contribute to planar growth and shrinkage alongside 1-D gliding clusters.

The diffusion coefficients (both along basal and prismatic planes) of each cascade-generated SIA

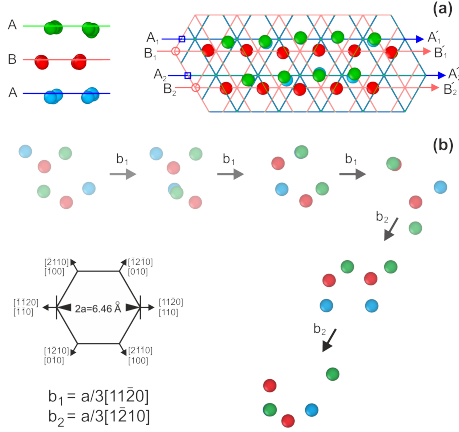


Figure 3: Graphical representation of an ADC. (a) Equivalent sphere analysis is used to demonstrate the configuration of a perfect 1-D glider from prismatic (left) and basal (right) view. As a result, off-site atoms are illustrated and the Burgers vector is drawn using the structural mesh. Here, three consecutive basal planes of an ADC with 6 SIAs are identified by letters A (blue), B (red) and A' (green) based on their position along the c axis. On each plane, 2 crowdions are identified along parallel directions, e.g. $\overline{A_1A_1'}$ and $\overline{A_2A_2'}$ on plane A. (b) Wigner-Seitz cell analysis is used to trace the gliding behaviour of a 2-D crowdion cluster containing 6 SIAs. Such SIA clusters can reconfigure themselves and change their direction of pure 1-D diffusion from one compact direction to another on the same plane.

cluster were estimated by tracking their size and position of their center of mass (see SM - section 4.4.2). D_c vs. D_a is illustrated in Fig. 4. Clusters with a diffusion coefficient lesser than $D_{mob} = 10^{-8}$ Å/ps were considered immobile. Single SIAs are shown by stars and characterized by D_a to D_c ratio of 1.13 and 0.89 for M2R and M3R, respectively. The diffusion coefficients of cascade-induced SIA clusters are higher than those of SIA clusters created by agglomeration, more remarkably for M3R (see SM - section 4.4.2). This indicates defects created during extreme out-of-equilibrium conditions can differ substantially from those produced in near-equilibrium conditions [42]. Clusters created by the interaction of subcascade shockwaves have a higher propensity to lead to crowdion formation than the aggregation of point defects. Furthermore, the stress fields induced by the cascade debris may also play a role; such interactions are known to have an important effect on the kinetics of defects [43, 44, 45, 46, 47, 48, 49].

Using the same bias factor threshold as previously, we classified SIA clusters into three groups: a-biased diffusing clusters (ADC), isotropically dif-

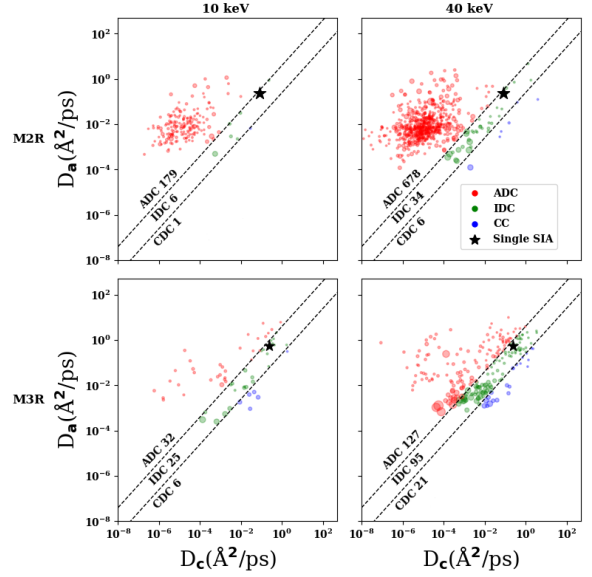


Figure 4: Diffusion coefficients of cascade-induced SIA clusters. Calculations were performed using the M2R and M3R potentials. Two PKA energy of 10 and 40 keV are illustrated (20 and 30 keV results available in the S.I.). Each dot represents one SIA cluster and the star markers show the single SIAs. Data are color-coded based on the ratio of D_a/D_c . The red colored points can be interpreted as ADCs, the green colored dots can be interpreted as roughly isotropically diffusing SIA clusters, and the blue colored dots can be interpreted as climbing clusters. The dashed lines bound the diffusion coefficients along the basal and prismatic planes where diffusion is considered to be isotropic (i.e. bias factor less than 25%).

fusing clusters (IDC), and c-biased diffusing clusters (CDC). SIACB model is based on the diffusion anisotropy of clusters, and their preferential interaction with different sinks. Therefore, in addition to 1-D gliders that were initially considered by the SIACB model, we include all ADCs to calculate n^g and ε^g . As can be seen in Fig. 2 (c), n^g is highly sensitive on the choice of force-field, but roughly independent of the PKA energy. The average size of ADCs is found to be in the same range of the cluster average size. The migration behavior of small clusters is known to be highly sensitive to the choice of force-field (see, e.g. Ref. [25]). In particular, the anisotropy of diffusion of M2R di-SIAs (SIA clusters of size 2) is very large, but M3R di-SIAs are nearly isotropic. Furthermore, M2R cascades tend to generate many more di-SIAs than M3R cascades. Hence, using M2R and accounting for di-SIAs would lead to a very large estimate of ε^g (≈ 0.62). However, both the large production rate

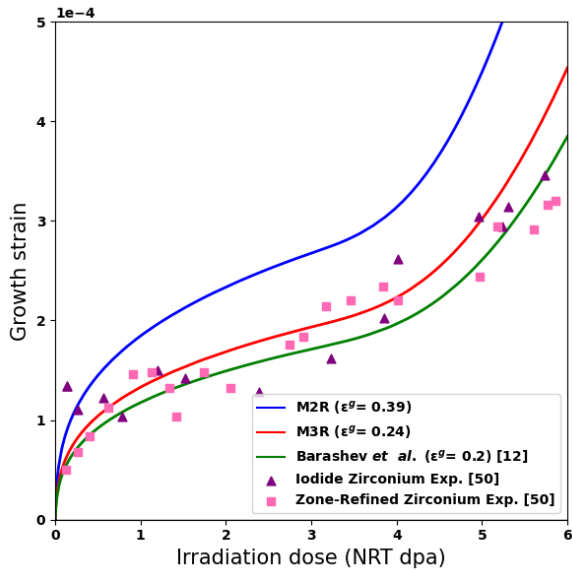


Figure 5: Rate theory prediction of prismatic RIG in Zr using ε^g calculated for the M2R- and M3R-based collision cascade simulations as compared to Barashev *et al.*'s SIACB model and experimental results [12, 50]. In this model, growth strain is measured against displacement per atom (DPA) in the procedure suggested by Norgett-Robinson-Torrens model (NRT) [51].

of di-SIAs and their large anisotropy of diffusion may be spurious. For this reason, we opted to exclude di-SIAs clusters from the analysis presented below, which can be viewed as a conservative lower bound estimate of ε^g . Estimates including di-SIAs are available in the SM - section 6. Our M2R simulations are associated with $\varepsilon^g \approx 0.39$, while M3R simulations are associated to 0.24. These values are based on an automated analysis of the SIA clusters; visual analysis leads to a value of 0.2. This compares to about 0.25 as estimated in Ref. [19] using an older force-field [52]. The SIACB [53, 13] model assumes a value of 0.2. Our calculations indicate ε^g is roughly independent of PKA energy (see SM - section 6).

A sensitivity analysis of the SIACB model was performed by inputting the calculated ε^g and n^g values for M2R and M3R into our own implementation of the model [12, 13]. formulation of the model and its parameters are available in the SM - section 9. Fig. 5 illustrates these outcomes for prismatic strain. The choice of force-field has a material effect on ε^g and n^g , but both estimates lead to a-type growth strains in broad agreement with experiments. However, negative strains along

the prismatic directions are overestimated by the model, as compared to experimentally measured values (see SM - section 9). Note rate-theory has a much larger effective timestep than MD. ε^g would therefore also include some amount of annealing of cascade debris to more accurately estimate ε^g . As shown in the SM - section 7, ε^g can increase as a function of annealing time. This suggests accelerated methods, such as object kinetic Monte Carlo (kMC) or on-the-fly kMC, can help get more accurate estimates of ε^g .

In conclusion, more likely than not, anisotropy of diffusion of cascade-induced SIA clusters is sufficient to explain RIG, but quantitative ambiguities remain given the sensitivity of our calculations to the choice of force-field. Also, *a contrario* SIACB theory, we observed few perfect 1-D gliders and many 2-D gliders, which could materially contribute to growth.

Our simulations highlight the importance of developing high-fidelity force-fields with a focus on describing the energetics and kinetics of defects and defect clusters in Zr. Furthermore, our calculations suggest that the anisotropy of cascade-induced SIA clusters is greater than that of clusters formed by agglomeration of individual SIAs, which may in part explain why ion and neutron irradiation leads to greater RIG than electron irradiation.

This work was supported by the Natural Sciences and Engineering Research Council of Canada (NSERC), and Atomic Energy of Canada Limited, under the auspices of the Federal Nuclear Science and Technology Program. The authors thank the Centre for Advanced Computing (CAC) at Queen's University and the Digital Research Alliance of Canada, formerly known as Compute Canada, for the generous allocation of computer resources.

References

- [1] S. I. Choi, J. H. Kim, Radiation-induced dislocation and growth behavior of zirconium and zirconium alloys—a review, *Nuclear engineering and technology* 45 (3) (2013) 385–392.
- [2] R. Holt, In-reactor deformation of cold-worked zr–2.5 nb pressure tubes, *Journal of Nuclear Materials* 372 (2–3) (2008) 182–214.
- [3] C. Woo, Modeling irradiation growth of zirconium and its alloys, *Radiation effects and defects in solids* 144 (1–4) (1998) 145–169.
- [4] B. Christiaen, C. Domain, L. Thuinet, A. Ambard, A. Legris, Influence of vacancy diffusional anisotropy: Understanding the growth of zirconium alloys under irradiation and their microstructure evolution, *Acta Materialia* 195 (2020) 631–644.

- [5] R. Holt, Mechanisms of irradiation growth of alpha-zirconium alloys, *Journal of Nuclear Materials* 159 (1988) 310–338.
- [6] Y. Li, N. Ghoniem, Cluster dynamics modeling of irradiation growth in single crystal zirconium, *Journal of Nuclear Materials* 540 (2020) 152312.
- [7] B. Christiaen, C. Domain, L. Thuinet, A. Ambard, A. Legris, A new scenario for vacancy loop formation in zirconium based on atomic-scale modeling, *Acta Materialia* 179 (2019) 93–106.
- [8] S. Pugh, Properties of reactor materials and the effects of radiation damage: Proceedings of the international conference held at Berkeley Castle, Gloucestershire, England, 30 May–2 June 1961. *dj littler (ed.)*, Butterworths, London, 1962, £ 6 6s (1963).
- [9] C. Woo, Theory of irradiation deformation in non-cubic metals: effects of anisotropic diffusion, *Journal of Nuclear Materials* 159 (1988) 237–256.
- [10] R. Holt, C. Woo, C. Chow, Production bias—a potential driving force for irradiation growth, *Journal of Nuclear Materials* 205 (1993) 293–300.
- [11] G. D. Samolyuk, A. V. Barashev, S. I. Golubov, Y. Osetsky, R. E. Stoller, Analysis of the anisotropy of point defect diffusion in hcp zirconium, *Acta Materialia* 78 (2014) 173–180.
- [12] A. V. Barashev, S. I. Golubov, R. E. Stoller, Theoretical investigation of microstructure evolution and deformation of zirconium under neutron irradiation, *Journal of Nuclear Materials* 461 (2015) 85–94.
- [13] S. I. Golubov, A. V. Barashev, R. E. Stoller, B. Singh, Breakthrough in understanding radiation growth of zirconium, *Tech. rep.*, Oak Ridge National Lab. (ORNL), Oak Ridge, TN (United States) (2014).
- [14] S.-M. Liu, I. J. Beyerlein, W.-Z. Han, Two-dimensional vacancy platelets as precursors for basal dislocation loops in hexagonal zirconium, *Nature communications* 11 (1) (2020) 1–8.
- [15] C. Dai, P. Saidi, M. Topping, L. Béland, Z. Yao, M. Daymond, A mechanism for basal vacancy loop formation in zirconium, *Scripta Materialia* 172 (2019) 72–76.
- [16] C. Dai, C. Varvenne, P. Saidi, Z. Yao, M. R. Daymond, L. K. Béland, Stability of vacancy and interstitial dislocation loops in α -zirconium: Atomistic calculations and continuum modelling, *Journal of Nuclear Materials* 554 (2021) 153059.
- [17] A. Harte, D. Jäderås, M. Topping, P. Frankel, C. Race, J. Romero, L. Hallstadius, E. C. Darby, M. Preuss, The effect of matrix chemistry on dislocation evolution in an irradiated zirconium alloy, *Acta Materialia* 130 (2017) 69–82.
- [18] C. Dai, Atomistic simulations of irradiation-induced dislocation loops in zirconium alloys, *Ph.D. thesis* (2018).
- [19] R. E. Voskoboinikov, Y. N. Osetsky, D. J. Bacon, Atomic-scale simulation of defect cluster formation in high-energy displacement cascades in zirconium (2006).
- [20] F. Gao, D. Bacon, L. Howe, C. So, Temperature-dependence of defect creation and clustering by displacement cascades in α -zirconium, *Journal of Nuclear Materials* 294 (3) (2001) 288–298.
- [21] R. Voskoboinikov, Y. N. Osetsky, D. Bacon, Identification and morphology of point defect clusters created in displacement cascades in α -zirconium, *Nuclear Instruments and Methods in Physics Research Section B: Beam Interactions with Materials and Atoms* 242 (1-2) (2006) 530–533.
- [22] B. Whiting, D. Bacon, Computer simulation of the migration of self-interstitial atoms in alpha-zirconium, *MRS online proceedings library* 439 (1) (1996) 389–394.
- [23] N. De Diego, Y. N. Osetsky, D. Bacon, Mobility of interstitial clusters in alpha-zirconium, *Metallurgical and materials transactions A* 33 (13) (2002) 783–789.
- [24] N. De Diego, A. Serra, D. Bacon, Y. N. Osetsky, On the structure and mobility of point defect clusters in alpha-zirconium: a comparison for two interatomic potential models, *Modelling and simulation in materials science and engineering* 19 (3) (2011) 035003.
- [25] J. F. March-Rico, B. D. Wirth, Defect cluster configurations and mobilities in α -Zr: A comparison of the bmd19 and m07 interatomic potentials, *Journal of Nuclear Materials* 559 (2022) 153441.
- [26] C. Maxwell, J. Pencer, E. Torres, Atomistic simulation study of clustering and evolution of irradiation-induced defects in zirconium, *Journal of Nuclear Materials* 531 (2020) 151979.
- [27] R. Stoller, A. Tamm, L. Béland, G. Samolyuk, G. Stocks, A. Caro, L. Slipchenko, Y. N. Osetsky, A. Aabloo, M. Klintonberg, et al., Impact of short-range forces on defect production from high-energy collisions, *Journal of chemical theory and computation* 12 (6) (2016) 2871–2879.
- [28] L. K. Béland, Y. N. Osetsky, R. E. Stoller, Atomistic material behavior at extreme pressures, *npj Computational Materials* 2 (1) (2016) 1–4.
- [29] L. K. Béland, A. Tamm, S. Mu, G. D. Samolyuk, Y. N. Osetsky, A. Aabloo, M. Klintonberg, A. Caro, R. E. Stoller, Accurate classical short-range forces for the study of collision cascades in Fe–Ni–Cr, *Computer Physics Communications* 219 (2017) 11–19.
- [30] J. Byggmästar, F. Granberg, K. Nordlund, Effects of the short-range repulsive potential on cascade damage in iron, *Journal of Nuclear Materials* 508 (2018) 530–539.
- [31] C. S. Becquart, A. De Backer, P. Olsson, C. Domain, Modelling the primary damage in Fe and W: Influence of the short range interactions on the cascade properties: Part 1—energy transfer, *Journal of Nuclear Materials* 547 (2021) 152816.
- [32] M. I. Mendeleev, G. J. Ackland, Development of an interatomic potential for the simulation of phase transformations in zirconium, *Philosophical Magazine Letters* 87 (5) (2007) 349–359.
- [33] A. P. Thompson, H. M. Aktulga, R. Berger, D. S. Bolintineanu, W. M. Brown, P. S. Crozier, P. J. in 't Veld, A. Kohlmeyer, S. G. Moore, T. D. Nguyen, R. Shan, M. J. Stevens, J. Tranchida, C. Trott, S. J. Plimpton, LAMMPS - a flexible simulation tool for particle-based materials modeling at the atomic, meso, and continuum scales, *Comp. Phys. Comm.* 271 (2022) 108171. doi:10.1016/j.cpc.2021.108171.
- [34] P. Saidi, Z. Wang, Y. Mao, L. K. Béland, Z. Yao, M. R. Daymond, A method for calculation of bias factor in anisotropic mediums, application to α -zirconium, *Journal of Nuclear Materials* 528 (2020) 151882.
- [35] A. Stukowski, Visualization and analysis of atomistic simulation data with OVITO—the Open Visualization Tool, *MODELLING AND SIMULATION IN MATERIALS SCIENCE AND ENGINEERING* 18 (1) (JAN 2010). doi:10.1088/0965-0393/18/1/015012.
- [36] K. Nordlund, S. J. Zinkle, A. E. Sand, F. Granberg,

- R. S. Averback, R. Stoller, T. Suzudo, L. Malerba, F. Banhart, W. J. Weber, et al., Improving atomic displacement and replacement calculations with physically realistic damage models, *Nature communications* 9 (1) (2018) 1–8.
- [37] Q. Yang, P. Olsson, Full energy range primary radiation damage model, *Physical Review Materials* 5 (7) (2021) 073602.
- [38] M. Mendeleev, M. Kramer, S. Hao, K. Ho, C. Wang, Development of interatomic potentials appropriate for simulation of liquid and glass properties of nizr2 alloy, *Philosophical Magazine* 92 (35) (2012) 4454–4469.
- [39] S. Wilson, M. Mendeleev, Anisotropy of the solid–liquid interface properties of the ni–zr b33 phase from molecular dynamics simulation, *Philosophical Magazine* 95 (2) (2015) 224–241.
- [40] X. Yang, X. Zeng, L. Chen, Y. Guo, H. Chen, F. Wang, Molecular dynamics simulations of the primary irradiation damage in zirconium, *Nuclear Instruments and Methods in Physics Research Section B: Beam Interactions with Materials and Atoms* 436 (2018) 92–98.
- [41] D. Terentyev, C. Lagerstedt, P. Olsson, K. Nordlund, J. Wallenius, C. S. Becquart, L. Malerba, Effect of the interatomic potential on the features of displacement cascades in α -fe: A molecular dynamics study, *Journal of nuclear materials* 351 (1-3) (2006) 65–77.
- [42] A. Calder, D. J. Bacon, A. V. Barashev, Y. N. Osetsky, On the origin of large interstitial clusters in displacement cascades, *Philosophical Magazine* 90 (7-8) (2010) 863–884.
- [43] L. K. Béland, Y. Anahory, D. Smeets, M. Guihard, P. Brommer, J.-F. Joly, J.-C. Pothier, L. J. Lewis, N. Mousseau, F. Schiettekatte, Replenish and relax: Explaining logarithmic annealing in ion-implanted c-si, *Physical review letters* 111 (10) (2013) 105502.
- [44] L. K. Béland, N. Mousseau, Long-time relaxation of ion-bombarded silicon studied with the kinetic activation-relaxation technique: Microscopic description of slow aging in a disordered system, *Physical Review B* 88 (21) (2013) 214201.
- [45] L. K. Béland, Y. N. Osetsky, R. E. Stoller, H. Xu, Kinetic activation–relaxation technique and self-evolving atomistic kinetic monte carlo: Comparison of on-the-fly kinetic monte carlo algorithms, *Computational Materials Science* 100 (2015) 124–134.
- [46] P. Brommer, L. K. Béland, J.-F. Joly, N. Mousseau, Understanding long-time vacancy aggregation in iron: A kinetic activation-relaxation technique study, *Physical Review B* 90 (13) (2014) 134109.
- [47] L. K. Béland, Y. N. Osetsky, R. E. Stoller, H. Xu, Slow relaxation of cascade-induced defects in fe, *Physical Review B* 91 (5) (2015) 054108.
- [48] L. K. Béland, G. D. Samolyuk, R. E. Stoller, Differences in the accumulation of ion-beam damage in ni and nife explained by atomistic simulations, *Journal of Alloys and Compounds* 662 (2016) 415–420.
- [49] A. Barashev, S. Golubov, H. Trinkaus, Reaction kinetics of glissile interstitial clusters in a crystal containing voids and dislocations, *Philosophical Magazine A* 81 (10) (2001) 2515–2532.
- [50] G. Carpenter, R. Zee, A. Rogerson, Irradiation growth of zirconium single crystals: A review, *Journal of Nuclear Materials* 159 (1988) 86–100.
- [51] M. Norgett, M. Robinson, I. Torrens, A proposed method of calculating displacement dose rates, *Nuclear Engineering and Design* 33 (1) (1975) 50–54. doi: [https://doi.org/10.1016/0029-5493\(75\)90035-7](https://doi.org/10.1016/0029-5493(75)90035-7). URL <https://www.sciencedirect.com/science/article/pii/0029549375900357>
- [52] G. Ackland, S. Wooding, D. Bacon, Defect, surface and displacement-threshold properties of α -zirconium simulated with a many-body potential, *Philosophical Magazine A* 71 (3) (1995) 553–565.
- [53] A. V. Barashev, S. I. Golubov, R. E. Stoller, Theoretical investigation of microstructure evolution and deformation of zirconium under cascade damage conditions, ORNL/TM-2012 225 (2012).